REPORT DOCUMENTATION PAGE

Form Approved
OMB No. 074-0188

1. AGENCY USE ONLY (Leave blank)	2. REPORT DATE	3. REPORT TYPE AND DATES COVERED
	1995	Global Biomass Burning June 29, 1995

4. TITLE AND SUBTITLE
Algorithm for the Retrieval of Fire Pixels from DMSP Operaltional Linescan System Data

5. FUNDING NUMBERS
N/A

6. AUTHOR(S)
C.D. Elvidge, H.W. Kroehl, E.A. Kihn, K.E. Baugh, E.R. Davis, Wei Min Hao

7. PERFORMING ORGANIZATION NAME(S) AND ADDRESS(ES)

Desert Research Institute and Nevada Agricultural Experiment Station
University of Nevada System
Reno, NV 89506

Solar-Terrestrial Physics Division
NOAA National Geophysical Data Center
325 Broadway
Boulder, CO 80303

Cooperative Institute for Research in Environmental Sciences
University of Colorado
Boulder, CO 80303

Intermountain Fire Sciences Laboratory
USDA Forest Service
Missoula, MT 59807

8. PERFORMING ORGANIZATION REPORT NUMBER
N/A

9. SPONSORING / MONITORING AGENCY NAME(S) AND ADDRESS(ES)
SERDP
901 North Stuart St. Suite 303
Arlington, VA 22203

10. SPONSORING / MONITORING AGENCY REPORT NUMBER
N/A

11. SUPPLEMENTARY NOTES
Chapter submitted to a book on "Global Biomass Burning" edited by Joel S. Levine. June 29, 1995. This work was supported in part by SERDP. The United States Government has a royalty-free license throughout the world in all copyrightable material contained herein. All other rights are reserved by the copyright owner.

12a. DISTRIBUTION / AVAILABILITY STATEMENT
Approved for public release: distribution is unlimited

12b. DISTRIBUTION CODE
A

13. ABSTRACT ***(Maximum 200 Words)***

In reviewing the literature, the earliest report we were able to find describing the observation of fire using a satellite sensor acquiring daily-global earth observations occurred when Croft (1973) described observing fires at night in Africa using "photographs" generated from the Defense Meteorological Satellite Program (DMSP) Operational Linescan System (OLS) visible band data. Croft (1978) was later able to use digital OLS data to observe fires, city lights and gas flares. The first systematic inventory of fires with OLS data was accomplished by Cahoon et al. (1992) who manually digitized fire points from film produced from nighttime OLS orbits over Africa.

Since 1972, the U.S. Department of Defense has maintained at least two DMSP platforms carrying OLS sensors in earth orbit. Because of the large data volume and restrictions on access to the data, a digital archive for DMSP-OLS data was not established until 1992. A film archive established in 1974 at the NOAA National Geophysical Data Center holds analog data from approximately 1.7 million OLS orbits acquired in the twenty years prior to 1992.

14. SUBJECT TERMS
SERDP, DMSP, OLS, NOAA

15. NUMBER OF PAGES
40

16. PRICE CODE
N/A

17. SECURITY CLASSIFICATION OF REPORT	18. SECURITY CLASSIFICATION OF THIS PAGE	19. SECURITY CLASSIFICATION OF ABSTRACT	20. LIMITATION OF ABSTRACT
unclass	unclass	unclass	UL

Algorithm for the Retrieval of Fire Pixels From DMSP Operational Linescan System Data

Christopher D. Elvidge
Desert Research Institute
and Nevada Agricultural Experiment Station
University of Nevada System
Reno, Nevada 89506
Tel. 303-497-6121 FAX 303-497-6513 Email: cde@ngdc.noaa.gov

Herbert W. Kroehl
Eric A. Kihn
Solar-Terrestrial Physics Division
NOAA National Geophysical Data Center
325 Broadway, Boulder, Colorado 80303

Kimberly E. Baugh
Ethan R. Davis
Cooperative Institute for Research in Environmental Sciences
University of Colorado, Boulder, Colorado 80303

Wei Min Hao
Intermountain Fire Sciences Laboratory
USDA Forest Service
Missoula, Montana 59807

Chapter submitted to a book on "Global Biomass Burning" edited by Joel S. Levine.

June 29, 1995

Introduction

Traveling in the Himalayan foothills near Darjeeling , India in May 1848, British naturalist Joseph Dalton Hooker (1855) wrote that "fires, invisible by day, are seen raging all around ... At night we were literally surrounded by them; some smouldering, ... others fitfully bursting forth, whilst others again stalked along with a steadily increasing and enlarging flame, shooting out great tongues of fire, which spared nothing as they advanced with irresistable might." While numerous accounts such as this provide vivid descriptions of fires, the recording of such events are too few and contain insufficient detail to provide a basis for estimating the impact of biomass burning on greenhouse gas emissions or biodiversity. Daily satellite observations provide the only technical means for deriving the systematic global database on fire locations, dates and sizes required to meet current scientific requirements.

In reviewing the literature, the earliest report we were able to find describing the observation of fire using a satellite sensor acquiring daily - global earth observations occurred when Croft (1973) described observing fires at night in Africa using "photographs" generated from the Defense Meteorological Satellite Program (DMSP) Operational Linescan System (OLS) visible band data. Croft (1978) was later able to use digital OLS data to observe fires, city lights and gas flares. The first systematic inventory of fires with OLS data was accomplished by Cahoon et al. (1992) who manually digitized fire points from film produced from nighttime OLS orbits over Africa.

Since 1972, the U.S. Department of Defense has maintained at least two DMSP platforms carrying OLS sensors in earth orbit. Because of the large data volume and restrictions on access to the data, a digital archive for DMSP-OLS data was not established until 1992. A film archive established in 1974 at the NOAA National Geophysical Data Center holds analog data from approximately 1.7 million OLS orbits acquired in the twenty years prior to 1992.

With support from the Strategic Environmental Research and Development Program (SERDP), we have initiated the development of the algorithms and databases required for the detection of fires at night using digital OLS data. In this chapter we describe the algorithms we have developed and provide preliminary results on fire and associated greenhouse gas emission in southern hemisphere Africa.

The DMSP System: Sensors and Archive

The DMSP maintains a constellation of two satellites in sun-synchronous, near-polar orbit at altitudes of approximately 833 km, an inclination of 98.8 degrees, and an orbital period of 102 minutes. One satellite is in a dawn - dusk orbit, the second in a day - night orbit. The DMSP platforms are three axis stabilized, with roll, pitch, and yaw variations kept to within +/- 0.01 degrees. This stability is unique compared to other polar orbiting systems such as Landsat or the NOAA Polar Orbiting Environmental Satellites.

The currently orbiting DMSP satellites include F-12 with day-night overpasses at ~ 9:54 and 21:54 local time, F-13 with dawn-dusk overpasses at ~ 6:04 and 18:04.

The NOAA National Geophysical Data Center (NGDC) serves as DoD's archive of data for the DMSP sensors. The U.S. Air Force Global Weather Central has sends DMSP data tapes to NGDC daily. The DMSP archive was established in March of 1992, and began receiving data on a daily basis in September of 1992 and has operated continuously since that time (Table 1). At NGDC the DMSP data are decompressed, deinterleaved into separate files for each sensor, and geolocated. NGDC has developed capabilities to recover DMSP data which have been corrupted by switched bits.

The NOAA-NGDC DMSP archives are unique in that data from all of the DMSP sensors are available. Several other programs receive subsets of the DMSP data stream. The DMSP suite of sensors making observation of the Earth and atmosphere includes four sensors which make Earth observations (Table 1).

The Operational Linescan System (OLS) is an oscillating scan radiometer designed for cloud imaging with two spectral bands (VIS and TIR) and a swath of 3000 km. There are two spatial resolution modes in which data can be acquired. The full resolution data, having nominal spatial resolution of 0.56 km, is referred to as "fine". On board averaging of five by five blocks of fine data produces "smooth" data with a nominal spatial resolution of 2.7 km. Most of the data received by NOAA-NGDC is in the smooth

spatial resolution mode. The "VIS" bandpass straddles the visible and near-infrared (VNIR) portion of the spectrum with a full-width-half-maximum (FWHM) of 0.58 - 0.91 um. The TIR band has a FWHM of 10.3 - 12.9 um. The TIR band is calibrated using an on-board blackbody source and views of deep space to provide 8 bit data with a temperature range of 190 to 310 degrees Kelvin, ideal for detecting and characterizing clouds. The wide swath widths provide for global coverage four times a day: dawn, day, dusk, night. The OLS produces 85% of the incoming DMSP data volume. NGDC recently improved its geolocation accuracy for the OLS data to +/- one pixel using physically based orbital mechanics and terrain correction algorithms. A set of algorithms have been developed for retrieving cloud cover, cloud type, and cloud height from OLS data (e.g. Gustafson et al., 1994). The OLS has been included on all recent DPSP satellites (F-10, F-11, F-12, and F-13).

The other three sensors are passive microwave systems with coarse spatial resolution. The Special Sensor Microwave Imager (SSM/I) is a seven channel, conical scanning radiometer, which measures the Earth's emitted radiation in four thermal microwave frequencies. The 22.2 Ghz channel is vertically polarized. Both horizontal and vertical polarization channels are acquired for the other three frequencies. A wide range of environmental products have been developed from SSM/I data (Hollinger, 1989 and 1991), including: ocean surface wind speed, ice area coverage, ice age, ice edge location, precipitation over water, precipitation over land, cloud amount, cloud water, integrated water vapor, land surface temperature, land surface type, soil moisture, and

snow water content. The Special Sensor Microwave Temperature Sounder (SSM/T-1) is a seven channel passive microwave sounder that measures atmospheric emissions in the 50 to 60 Ghz oxygen band at seven cross track scan positions for use in constructing vertical profiles of atmospheric temperature. The Special Sensor Microwave Water Vapor Profiler (SSM/T-2) is a five channel passive microwave sounder that measures atmospheric emissions from 91 to 183 Ghz . The SSM/T-2 data are used to derive vertical profiles of water vapor, including relative and specific humidity and water vapor mass (Boucher et al., 1992).

Fire Detection With DMSP-OLS Data

The algorithm we have developed for detection of fires in OLS data relies on detecting areas of active visible and near infrared emission on the planet surface at night, when solar illumination is absent. The VIS band signal is intensified at night using a photomultiplier tube (PMT), making it possible to detect faint VNIR emission sources. The PMT system was implemented to facilitate the detection of clouds at night using the visible band. With sunlight eliminated, the light intensification results in a unique data set in which city lights, gas flares, and fires can be observed.

One adverse effect of the light intensification is that the system is quite sensitive to scattered sunlight. Under certain geometric conditions, the OLS telescope is illuminated by sunlight. Scattering of sunlight off the end of the telescope into the optical path results

in visible band detector saturation, a condition referred to as glare (Figure 1). The exact shape and orbital position of the glare changes through the year, but is generally confined to the western side of nighttime orbits in the 40 to 60 degree latitude range (north and south). Because of the substantial orbital overlap in this latitude range, it is still possible to acquire nearly global coverages of glare free data each night.

Only the largest fires produce enough thermal emission in the 10-12 um region to be detected with the TIR band in smooth spatial resolution mode. At first this may seem counterintuitive to have better success at fire detection in the visible-NIR region than in the thermal region. There are several factors which contribute to the superior performance of the nighttime VIS data over the TIR data in "smooth" spatial resolution mode. First, the TIR band saturates at 310 K. Typical surface temperature backgrounds are in the 270 to 290 K range. Given the lack of contrast between the background and the 310 K limit, it takes a large number of saturated fine pixels to yield a discernable temperature anomaly in a smooth TIR pixel. Another factor is the expansion of the Instantaneous Field of View (IFOV) which occurs when the VIS band signal is intensified with the PMT. The IFOV of the individual "fine" pixels under PMT operating conditions is approximately 1.74 km. The IFOV of the resulting "smooth" VIS band data at night is 3.98 km (center to center the smooth pixels are ~2.7 km apart). There is substantial overlap between adjacent VIS band "fine" pixels. As a result, a subpixel sized fire bright enough to saturate a "fine" pixel in the VIS band will generally be observed in at least two and can potentially be observed in up to six of the 25 pixels which get averaged into a

"smooth" pixel (see chapter by Kihn in this volume). The result is that there is a variable amount of "double-counting" of fires in the nighttime visible. Because of the smaller IFOV of the TIR "fine" pixels, there is little overlap between adjacent pixels and subpixel fires are generally observed only once. Finally, as described by Planck's Law, the overall spectral emission of a blackbody increases as temperature increases and there is a strong shift towards emission at shorter wavelengths. An examination of Planck curves of spectral emission for blackbodies ranging from 300 to 1000 K indicates that the VIS band (0.58 to 0.91 um) is in a better spectral position for detecting hot materials than the TIR band (10 to 12 um). A preliminary examination of "fine" spatial resolution TIR data suggests that fires can be detected in either daytime or nighttime conditions, but that many of the fire pixels will be saturated at 310 K.

Components of the Nighttime Fire Detection Algorithm

Suborbiting

OLS orbits are visually inspected to identify usable orbital segments. Suborbits are created for nighttime orbital segments over land areas. The suborbiting reduces the data volume which must be processed and is used to exclude features which such as auroras, which are not relevent to the detection of fires.

Glare Removal

OLS images are preprocessed to remove glare. Glare is detected when a 20 by 20 block of pixels is encountered with all pixels having saturated digital number (DN) counts

of 63. The detection of the saturated block of pixels initiates an expanding search for all adjacent pixels with DN counts of 45 or greater. The DN counts for these pixels are set to zero. The cell size of 20 by 20 for glare detection was selected to avoid mistaking large cities as glare and to accomodate variations in glare size and shape. An example of OLS glare removal is shown in Figure 2.

Identification of VNIR Emission Sources

Because of brightness variations which occur within and between orbits, it is not possible to set a single digital number (DN) threshold for identifying VNIR emission sources. We have developed software for detecting VNIR emission sources (lights) in nighttime OLS data using thresholds established based on the local background. This "light picking" algorithm operates using background DN statistics generated from 50 by 50 pixel cells. Lights are identified in the central 20 by 20 pixel block inside the 50 by 50 pixel block used to generate the background statistics. Processing of an image proceeds by tiling the results from adjacent 20 by 20 pixel cells.

The nested configuration of the 20 by 20 cell inside of the 50 by 50 cell was designed to provide rapid processing of suborbits and to accomodate changes in background brightness. Identifying the local threshold for a 20 by 20 cell is 400 times faster than processing a new threshold for each individual pixel. This 20 by 20 pixel sizes matches the cell size used for glare detection. There is 60 % overlap between the 50 by 50 pixel outer cells used to generate background statistics. This results in smooth

transitions in threshold levels, avoiding threshold disparities between adjacent 20 by 20 pixel cells.

The distribution of DN values in each 50 by 50 pixel cell is analyzed to identify the set of pixels for use as the local backgound. VIS band DN values range from 0 to 63. Zeroes are missing data and 63's are saturated pixels. The lower limit of the background is taken to be DN=1. The upper limit of the background is determined using a frequency distribution of pixel counts versus DN values (Figure 3). Starting from DN=63 and working down, the frequency distribution is analyzed to detect the first DN value where five consecutive DN bins have greater than 0.4 % of the total pixel counts. For a full 50 by 50 cell, this corresponds to a search threshold of 10 pixels per DN bin. Once the upper limit of the background is selected, the mean and standard deviation of the background pixel set is calculated. Pixels containing VIS band emission sources are then identified using a threshold set at the DN value of the background mean plus three standard deviations. Figures 4, 5, and 6 show examples of the light picker results applied to nighttime OLS imagery of Africa. Figure 7 shows the locations of lights which were detected in an OLS suborbit covering a large part of southern hemisphere Africa on September 18, 1992.

Lightning Removal

If an OLS line scan tracks across a cloud illuminated by lightning, a linear feature is produced which can be detected using the light picking algorithm described above.

Typically the lighting is observed in one or two scan lines, but can occur in up to three or four scanlines if multiple lightning strikes continue to illuminate the same cloud mass. We identify and remove lighting features from the images produced by the light picking algorithm by testing the length versus width of all lights detected in cloud areas. Clouds are identified using the TIR band.

Geolocation

Our geolocation algorithm operates in the forward mode, projecting the center point of each pixel onto the Earth's surface. The geolocation algorithm estimates the latitude and longitude of pixel centers based on the geodetic subtrack of the satellite orbit, satellite altitude, sensor model, an Earth sea level model, and digital terrain data. The geodetic subtrack of each orbit is modeled using daily radar bevel vector sightings of the satellite (provided by Naval Space Command) as input into an Air Force orbital mechanics model that calculates the satellite position every 0.4208 seconds. The satellite heading is estimated by computing the tangent to the orbital subtrack. Satellite attitude is stabilized using four gyroscopes (three axis stabilization), a star mapper, Earth limb sensor and a solar detector. The sensor model was developed based on the instrument mounting, scan characteristics, and the integration times for A/D converison. We have used an oblate ellipsoid model of sea level and have used Terrain Base (Row and Hastings, 1995) as a source of digital terrain elevations.

Identification of Stable Lights

Image time series analysis is used to identify stable lights produced by cities, towns, and industrial facilities. Heavy cloud cover blocks the detection of VNIR emission sources and light cloud cover tends to diffuse lights present on the Earth's surface, making them appear larger than their actual size. In developing a stable lights dataset we establish a reference grid and process large numbers of orbits, classifying pixels into one of three catagories: 1) cloud, 2) cloud-free with no VNIR emission source, and 3) cloud-free with a VNIR emission source. Following classification, pixels are geolocated and resampled into the reference grid. The time series analysis is accomplished by running a counter for each of the three classes for each cell in the reference grid. In this way it is possible to identify which grid cells contain stable lights and also which areas need additional observations due to cloud cover. The stable lights for the southern hemisphere Africa derived from 96 orbits of data are shown in Figure 8.

We have compared the OLS stable lights against the populated place lines from the Defense Mapping Agency (DMA) Digital Chart of the World (DCW) for several regions. The DCW populated place lines were digitized from DMA Operational Navigation Charts (ONC) and are widely used as a source of geographic information on the global distribution of cities. The comparison was made to determine if it would be possible to use the DCW populated place lines as a surrogate for OLS stable lights. While the OLS stable lights covered each of the DCW populated place line features, a large number of OLS stable lights were not identified with DCW populated place lines (see Figure 9).

These results indicate that it would not be possible to use the DCW populated place lines in place of the empirical determination of OLS stable lights using the time series analysis.

Identification of Fires

Fires are identified as VNIR emission sources that are not associated with either stable lights or lightning. Lightning is screened out of the incoming data stream immediately after the light picking algorithm is applied. Stable lights are masked out of the incoming data after the lights have been geolocated and resampled to the same reference grid as the stable lights dataset. The algorithm that removes the stable lights identifies all pixels which occur in or directly adjacent to the known stable light locations and sets their DN values to zero. The remaining pixels, which contain ephemeral VIS band emission sources are taken to be fires. Figure 10 shows the fires which were detected from the September 18, 1992 orbit of southern hemisphere Africa shown in Figure 7 after masking out of stable lights (Figure 8) and lightning. By compiling burn observations from adjacent orbits over specific time intervals it is possible to assemble continental scale depictions of the spatial and temporal patterns of biomass burning. Figure 11 shows the cumulative burn observations from a three night - six orbit period in southern hemisphere Africa, covering September 18, 19, and 20, 1992.

Calibration of Burn Area

Because the OLS sensor can detect fires which are sub-pixel in size, it cannot be assumed that the entire area of a pixel with a fire has been burnt. In estimating the

cumulative burn area during a fire season it is reasonable to assume that an area only burns once, despite the fact that fires may be observed for multiple days in the same location. In order to calibrate burn areas it is necessary to have another source of data. Field surveys are generally only feasible to validate burn areas for a small number of fires in a limited area. Procedures have been developed for using Landsat data to develop regionally applicable calibrations of burn area for AVHRR fire observations (Scholes et al., 1994). However, the acquisition of Landsat style data in many parts of the world remains problematic, the data costs are high and the processing requirments are intensive.

Early results obtained from simultaneously acquired nighttime OLS data in "smooth" and "fine" spatial resolution modes suggests that it may be feasible to calibrate OLS burn areas based on a temporal subsampling of OLS fine data. Fine resolution OLS data can be acquired using a direct readout ground receiving station or by using the on-board tape recorders. The smooth resolution data continues to be produced even when the on-board tape recorders are used to acquire fine resolution data.

Figure 12 shows a nighttime OLS data of fires in Sudan on December 7, 1994 in both the "smooth" and "fine" spatial resolution modes. With the increased spatial resoultion of the "fine" data it should be possible to make an improved estimated of the area of active fire. By using a temporal sub-sample of "fine" resolution data, it may be possible to develop regionally valid burn area estimates which could be applied to nightly data acquired in the "smooth" spatial resolution mode.

APPLICATIONS

Estimation of Trace Gas and Particulate Matter Emissions

One of the major applications of satellite based biomass burning observations is to estimate of trace gas and particulate emissions. To demonstrate the feasability of using DMSP-OLS fire observations to estimate the emissions of important trace gases and particulate matter from biomass burning, the USDA Forest Service, Intermountain Fire Sciences Laboratory used the OLS fire observations presented in Figure 11 and estimated the resulting carbon dioxide emissions on a one degree grid. Because we have not developed a calibration to burn area for the Figure 11 fire observations, the carbon dioxide emission modelling was performed assuming that the entire area of each fire pixels was burnt. The results shown in Figure 13 are thus overestimates of the actual emissions which occurred during the three day period. More realistic estimates could be obtained with calibrated burn areas.

Biomass fires in the southern hemisphere Africa are mostly used for shifting cultivation, deforestation and savanna burning in this region. Other sources of biomass fires are fuelwood use and clearing of agricultural residues. The ecosystems consist of tropical evergreen forests, semi-evergreen forests, secondary forests, deciduous forests, woodland and grassland savannas, and arid savannas. The trace gases for which emissions can be estimated from the OLS fire observations include CO_2, CO, CH_4, C_2-C_6 alkanes, alkenes and alkynes, aromatic compounds (benzene, toluene, and xylenes), alcohols, aldehydes, ketones, organic acids, NO_x,

NH_3, N_2O, and cyanogen compounds. The particulate matter which can be estimated includes total particulate matter and particles less than 2.5 mm in diameter.

The amount (T) of a trace gas or aerosol particles X emitted from biomass burning per unit time in each pixel is estimated using the following equation:

$$T = M * EF X_a = A * B * \alpha * (EF X_f * P_f + EF X_s * P_s)$$

T: Amount of X produced from fires per unit time

M: Amount of biomass burned per unit time

$EF X_a$: Weighted-average emission factor of X

A: Area burned per unit time

B: Aboveground biomass density

α: Fraction of aboveground biomass burned

$EF\,X_f$: Emission factor of X during the flaming phase

$EF\,X_s$: Emission factor of X during the smoldering phase

P_f: Fraction of biomass burned during the flaming phase

P_s: Fraction of biomass burned during the smoldering phase

Note that the emission factors are a function of combustion efficiency:

$EF\,X_f = f(Ce_f)$ CE_f: combustion efficiency during the flaming phase

$EF\,X_s = f(Ce_s)$ CE_s: combustion efficiency during the smoldering phase

Further, combustion efficiency is function of factors related to meteorological and fuel conditions at the time of burning:

CE_f or $CE_s = f$(meteorological conditions; characteristics of biomass)

$= f$(wind velocity, temperature, humidity; amount, components, moisture

and elemental composition of biomass)

Currently many of the above factors are estimated based on coarse resolution vegetation maps, statistical estimates of above ground biomass density, and estimates of emission factors and generalized flaming versus smoldering combustion behaviors (Hao and Ward, 1993; Hao and Liu, 1994). The suite of DMSP microwave sensors have potential for estimating global precipitation which could be used with OLS surface temperatures estimates as input into vegetation growth models to make dynamic estimates of fuel loads and fuel conditions. The SSM/T2 water vapor profiles and SSM/T1 air temperature profiles could be used to estimate the near surface relative humidity, a key factor required to estimate the combustion efficiency.

Resource Management

The U.S. Government spends approximately $500 million in fighting wildfires each year. Losses in lives, property and resources are much higher. Fire fighters have long recognized that early detection of fires is key to cost-effective fire suppression and fire management. Fires which are not detected early have time to spread and become unmanageable, costly to fight, and result in great losses in lives, property and resources. Satellite sensors have a proven capability for the detection of fires. However, the infrastructure required to transmit fire locations observed by satellites to local entities engaged in fire fighting / fire management has not been widely developed.

The requirement for early detection of wildland fires goes beyond the protection of lives and property. Global conservation of biodiversity in the face of expanding human populations will require individual countries to manage and often restrict biomass burning. Satellite observations of fires can be used to evaluate the effectiveness of government programs to reduce the frequency or seasonal timing of biomass burning. As an example, in 1994 the government of Madagascar issue an "no-burn" edict in an attempt to reduce the widespread occurance of biomass burning. In retrospect, how effective was the edict? Figure 14 shows the nighttime fires which were detected with DMSP-OLS data for September 20, 1992 and 1994. While fires were not eliminated in 1994, there was a substantial reduction in the number of fires relative to 1992.

CONCLUSION

We present the first digital algorithm for nighttime fire detection with data from the DMSP-OLS, a set of preliminary results and examples of applications which can be made with the fire observations. The algorithm we have developed is still being refined and needs to be thoroughly tested. The early results indicate that it would be feasible to produce a systematic global survey of fires for the years 1992-95 using the DMSP archives held at NOAA-NGDC.

In addition to fire monitoring, the nighttime OLS data can be used to map the distribution of stable visible-NIR emission sources present on the Earth's surface. A global stable lights dataset may be of considerable value for use as a global urban land

cover class, filling in a gap in the current land cover mapping capabilities of sensors such as the NOAA-AVHRR. The global stable lights dataset would also be useful in refining the datasets on the distribution of population and the consumption of energy.

The DMSP-OLS has several advantages over currently available civil sensors for the daily monitoring of fires: 1) The positional stability of the OLS platform permits high accuracy geolocation of fires. 2) OLS provides superior spatial resolution (2.7 km pixels in "smooth" data and 0.56 km pixels in "fine" data). 3) Global coverages can be obtained without reliance on a network of receiving stations. 4) The nighttime VIS band intensification makes it possible to detect faint VNIR emission sources on the Earth's surface. 5) Because the OLS "smooth" data is a true average of 25 "fine" pixels, it is feasible to develop regionally valid "smooth" data burn area calibrations based on a temporal subsample of "fine" data. And 6) The DMSP series is expected to continue until 2005-2006 without interruption, thus providing the potential for 15 years of continuous global fire observations.

Current efforts at NOAA-NGDC are focussing on validating DMSP-OLS fire observations through participation in international biomass burning experiments, intercomparison of fire monitoring capabilities with other sensors, development of procedures for estimating burn area in 2.7 km resolution "smooth" OLS data with temporal subsamples of 0.56 km "fine" data, and installation of data lines for reception of near real-time OLS data for use in early detection of fires.

ACKNOWLEDGMENT

This project was supported by the Strategic Environmental Research and Development Program (SERDP).

REFERENCES

Boucher, D., B. Thomas, and V.J. Falcone, 1992, Performance of the DMSP Special Sensor Microwave Humidity Profiles: Preliminary Results. Proceedings of the First NMC/NESDIS/DOD Conference on DMSP Retrieval Products, R. Isaacs, E. Kalnay, G. Ohring, R. McClatchey (eds.), PL-TR-92-2191. pp. 17-24.

Cahoon, D.R. Jr., Stocks, B.J., Levine, J.S., Cofer, W.S. III, O'Neill, K.P., 1992, Seasonal distribution of African savanna fires. Nature, v. 359, p. 812-815.

Croft, T.A., 1973, Burning waste gas in oil fields. Nature, v. 245, p. 375-376.

Croft, T.A., 1979, The brightness of lights on Earth at night, digitally recorded by DMSP satellite. Stanford Research Institute Final Report Prepared for the U.S. Geological Survey.

Gustafson, G.B., R.G. Isaacs, R.P. d'Entremont, J.M. Sparrow, T.M. Hamill, C. Grassotti, D.W. Johnson, C.P. Sarkisian, D.C. Peduzzi, B.T. Pearson, V.D. Jakabhazy, J.S. Belfiore, and A.S. Lisa, 1994, Support of environmental requirements for cloud analysis and archive (SERCAA): Algorithm Descriptions. PL-TR-94-2114, Scientific Report #2, Phillips Laboratory, Directorate of Geophysics, AFMC, Hanscom AFB, MA 01731-3010.

Hao, W.M. and M.-H. Liu, 1994, Spatial and temporal distribution of tropical biomass burning. Global Geochemical Cycles, v. 8, p. 495-503.

Hao, W.M. and D.E. Ward, 1993, Methane production from global biomass burning. Journal of Geophysical Research, v. 98, no. 20, p. 657-661.

Hollinger, J., 1989, DMSP Special Sensor Microwave Imager Calibration/Validation. Naval Research Laboratory, Washington, D.C., Final Report Volume I.

Hollinger, J., 1991, DMSP Special Sensor Microwave Imager Calibration/Validation. Naval Research Laboratory, Washington, D.C., Final Report Volume II.

Hooker, J.D., 1855: "Himalayan Journals" John Murray, London.

Row, L.W. III and Hastings, D.A., 1995: TerrainBase Worldwide Digital Terrain Data, Documentation Manual and CD-ROM. NOAA National Geophysical Data Center, Boulder, Colorado, NGDC Publication KGRD 30, 185 pp.

Scholes, R.J., D.E. Ward, C.O. Justice, 1995, Emissions of trace gases and aerosol particles due to vegetation burning in southern-hemisphere Africa. Journal of Geophysical Research, In Press.

LIST OF FIGURES

Figure 8. Stable lights in southern hemisphere Africa, derived from 96 orbits of nighttime DMSP-OLS data.

Figure 9. DMSP-OLS stable lights for an area surrounding Harare, Zimbabwe. Populated place lines from the Digital Chart of the World (DCW) are shown in white.

Figure 10. Nighttime fires detected in southern hemisphere Africa on a single orbit acquired on September 18, 1992.

Figure 11. Nighttime fires detected in southern hemisphere Africa during six orbits acquired over three nights - September 18-20, 1992.

Figure 12. Smooth (2.7 km) versus fine (0.56 km) resolution DMSP-OLS data of fires in southern Sudan, December 7, 1994.

Figure 13. Carbon dioxide emissions from biomass burning in southern hemisphere Africa based on DMSP-OLS fire observations from September 18 - 20, 1992.

Figure 14. Effect of 1994 government "no-burn" edict in Madagascar on nighttime fires observed with DMSP-OLS data.

Table 1
Defense Meteorological Satellite Program (DMSP)
Sensor Characteristics

Sensor	Wavelengths/Frequencies		Resolution	Swath Width
OLS	VIS = 0.58 -0.91 um TIR = 10.5 - 12.6 um		Fine = 0.56 km Smooth = 2.7 km	~~3600~~ 3000 km
SSM/I	Microwave Radiometer			
	19 GHz	H & V	70 X 45 km	1400 km
	22 GHz	V	60 X 40 km	
	37 GHz	H & V	38 X 30 km	
	85 GHz	H & V	16 X 14 km	
SSM/T1	Temperature Sounder			
	Seven from 50 - 60 GHz		174 km	1400 km
SSM/T2	Water Vapor Sounder			
	Five from 90 to 183 GHz		46 to 120 km	1400 km

Figure 1. DMSP-OLS nighttime image of the western USA showing glare. Orbit F1017618, April 16, 1994.

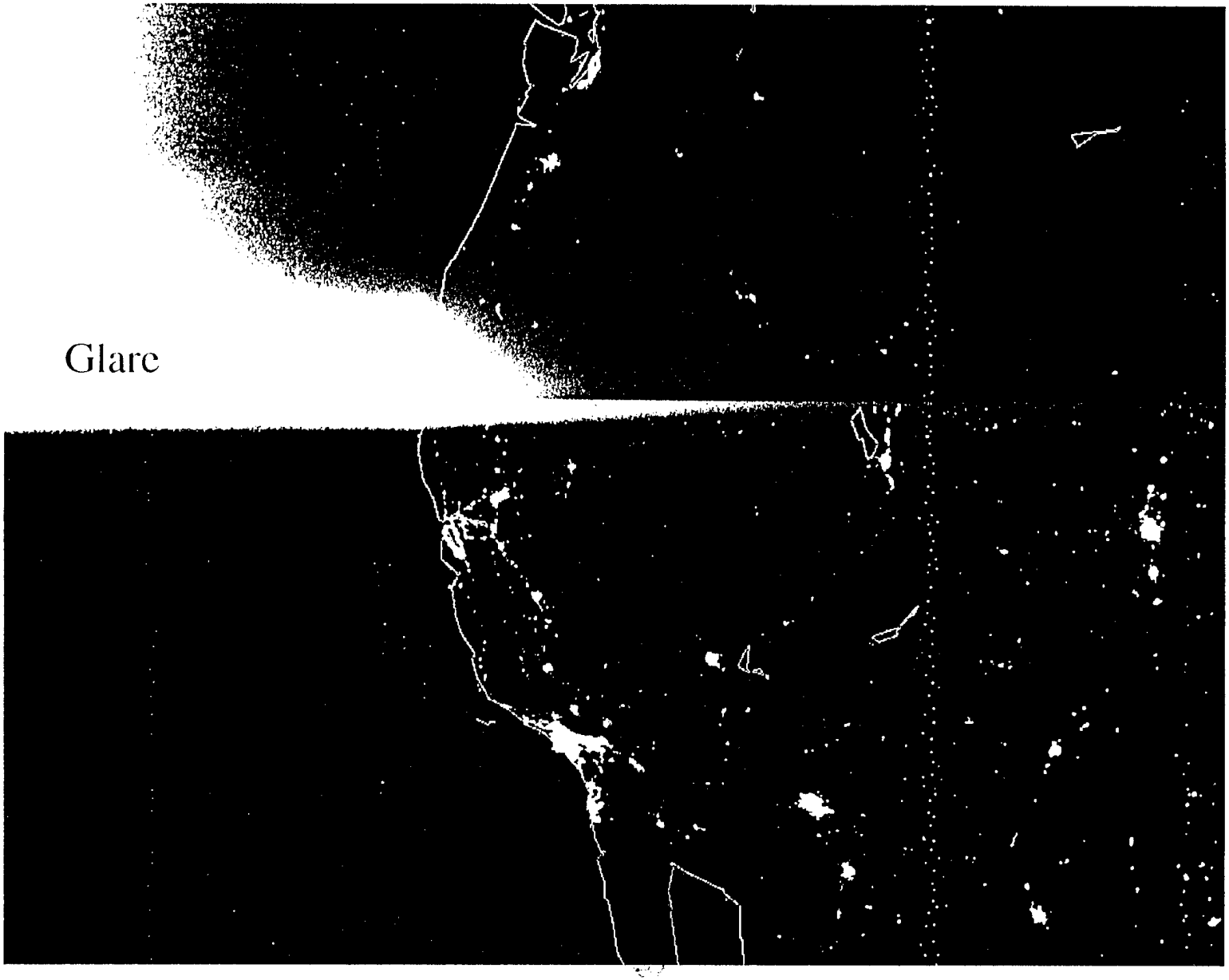

Figure 2. DMSP-OLS nighttime image of the western USA showing glare removed (compare to Figure 1). Orbit F1017618, April 16, 1994.

Figure 3. Histogram frequency distribution analysis to set local threshold for DMSP-OLS light detection.

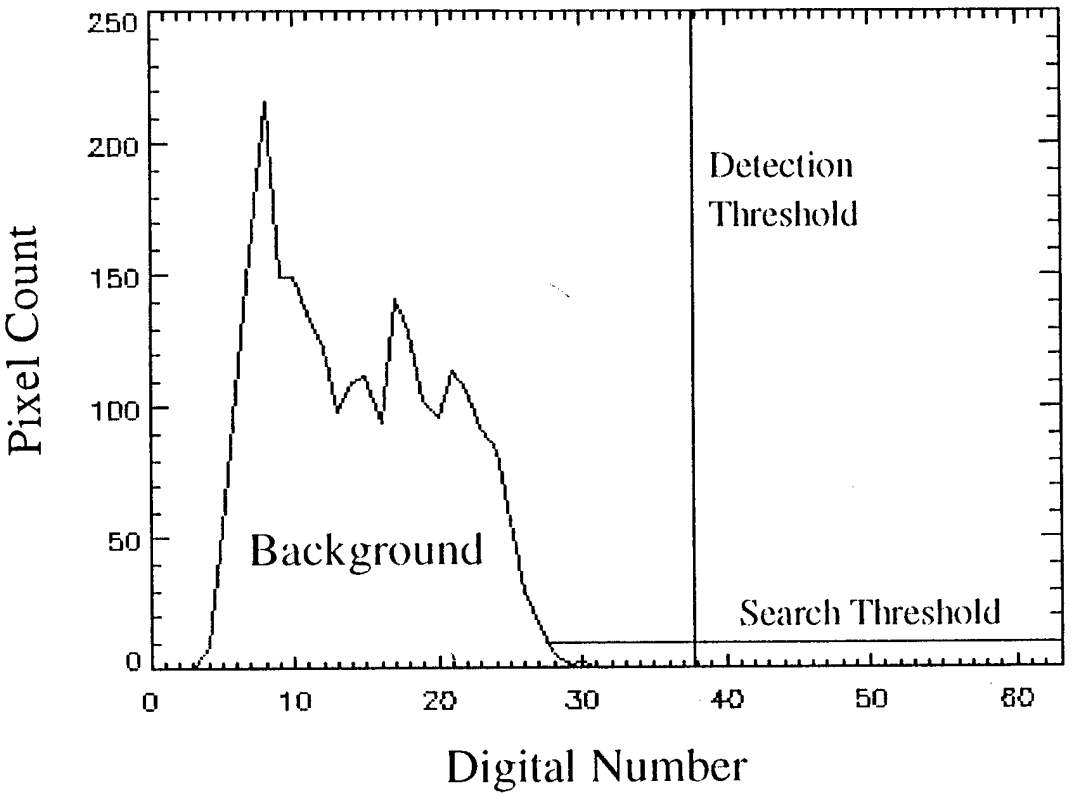

Figure 4. DMSP-OLS light picker - lights detected in presense of light cloud cover.

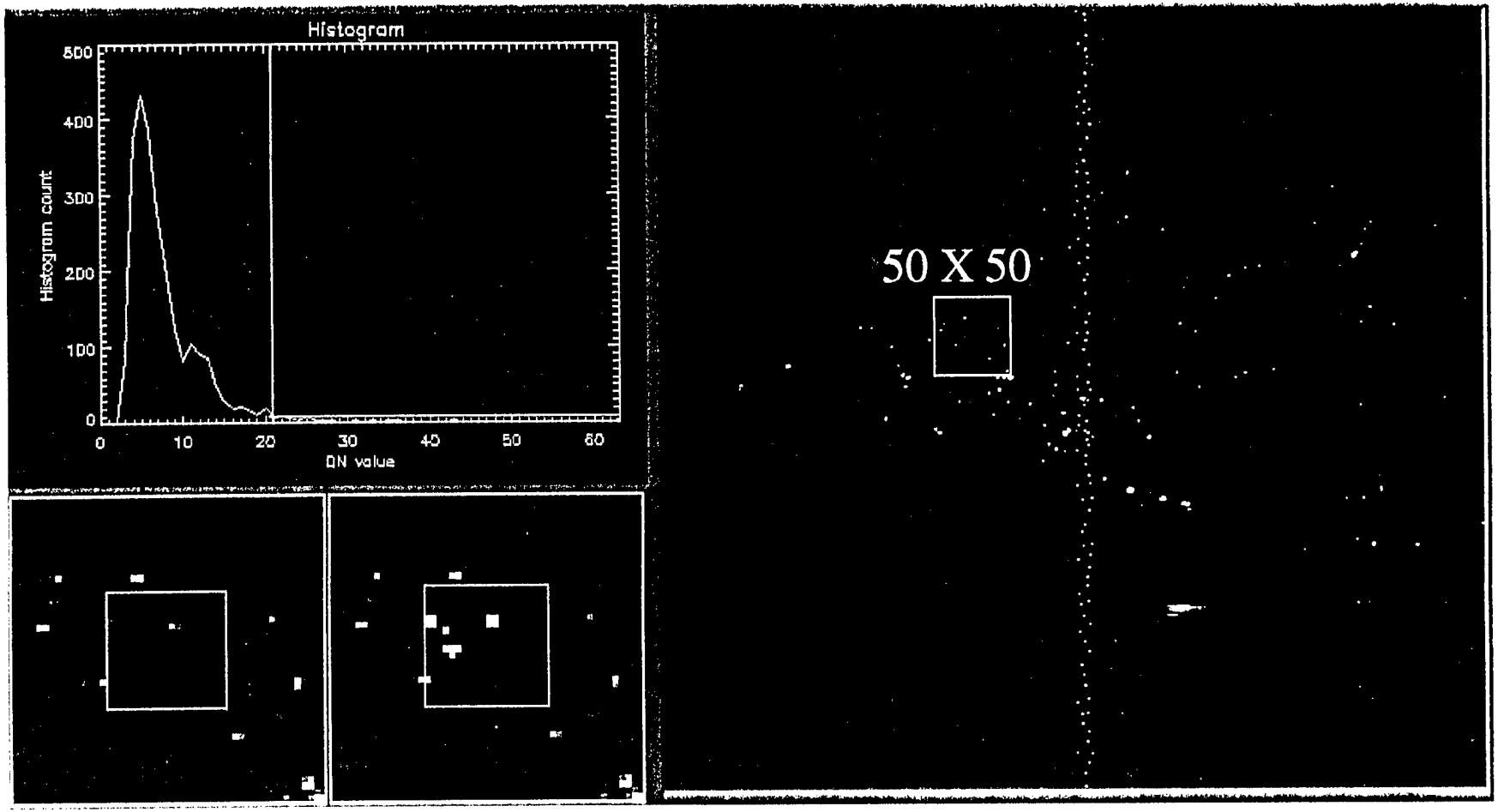

50 X 50 Raw Data

Lights Detected In 20 X 20 Interior Cell

Figure 5. DMSP-OLS light picker - lights detected in presense of heavy cloud cover.

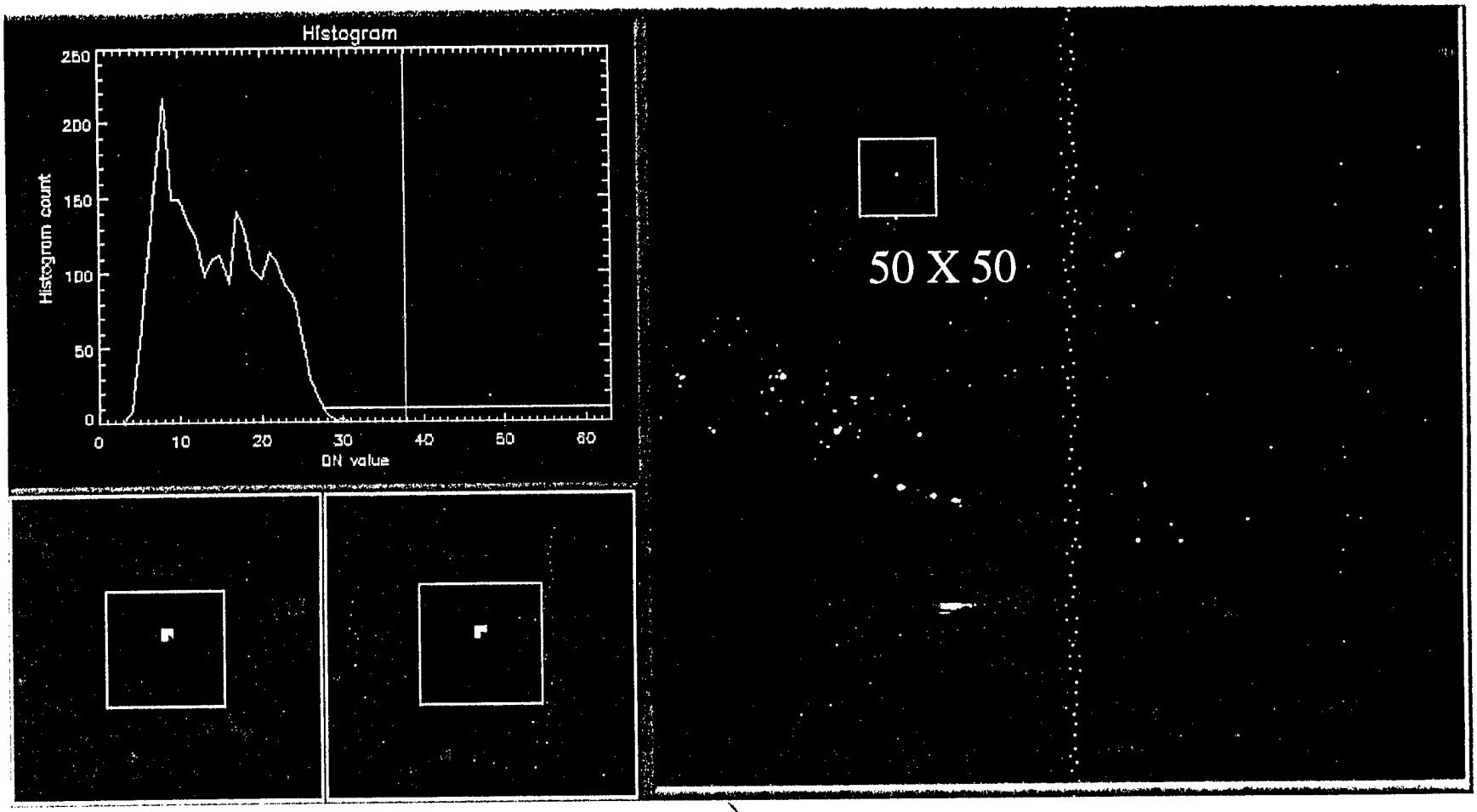

Figure 6. DMSP-OLS light picker applied to moon illuminated cloud cover with no VNIR emission sources detected.

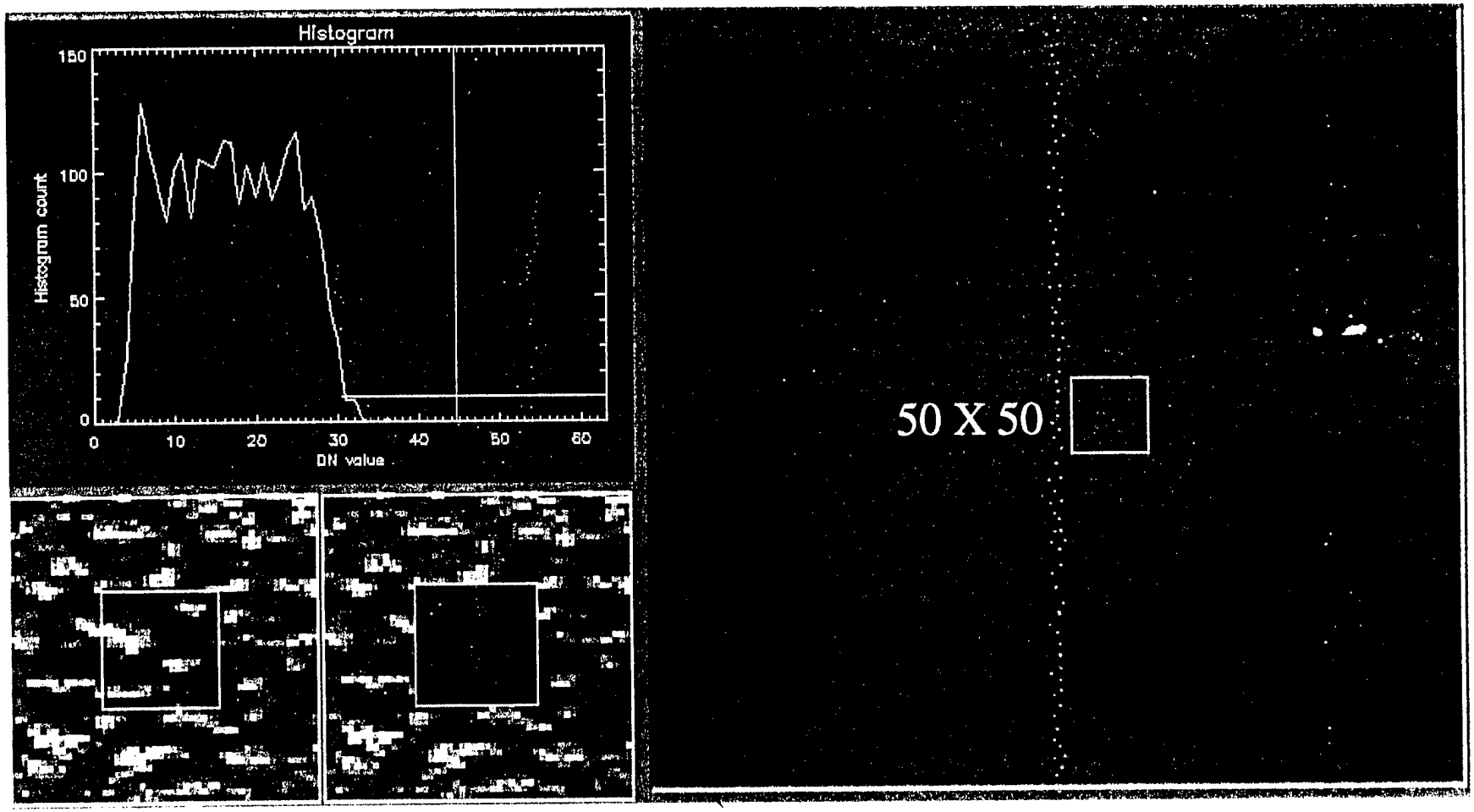

Figure 7. Lights (VNIR emission sources) detected in southern hemisphere Africa from a single DMSP-OLS orbit - September 18, 1992.

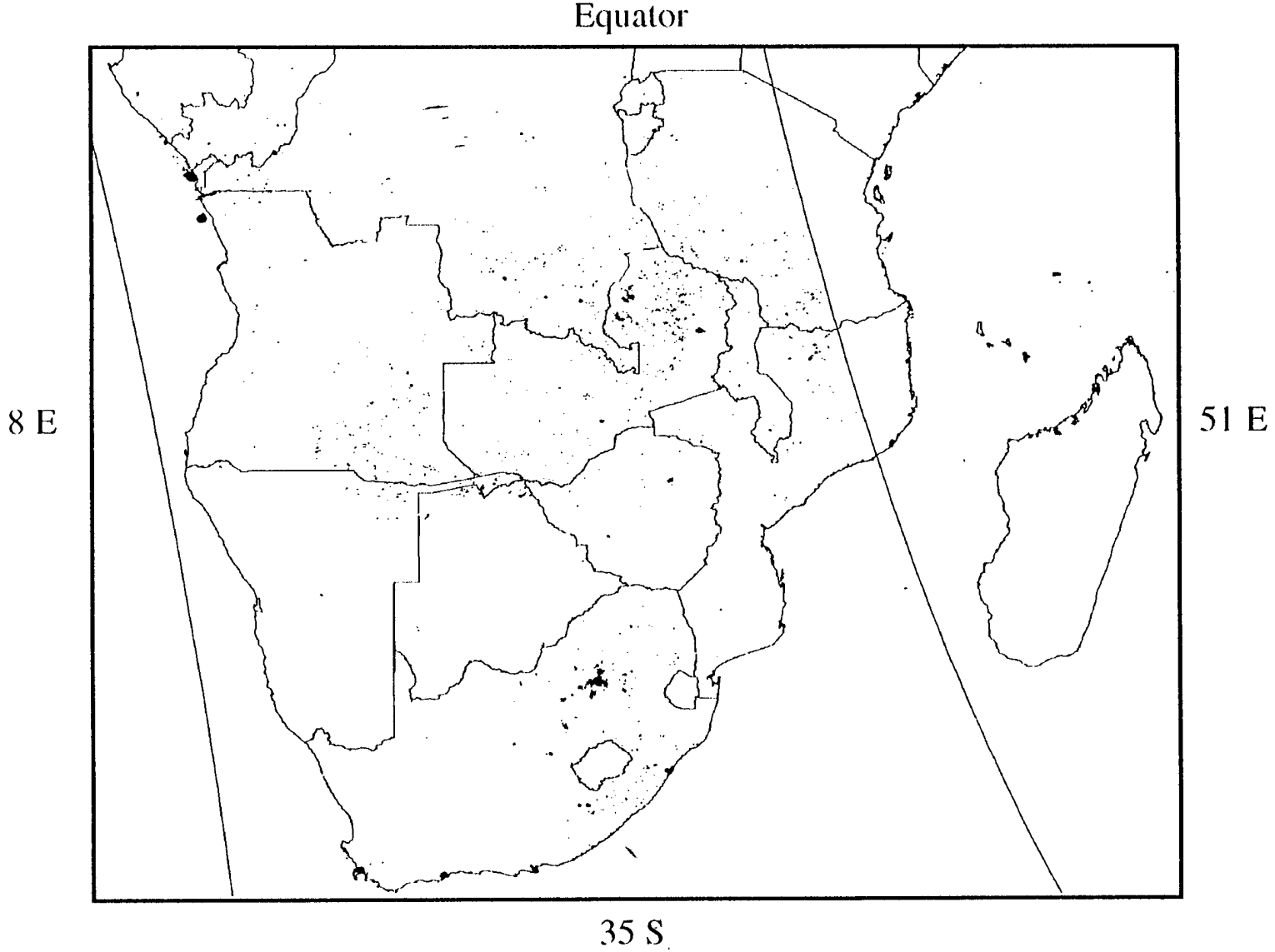

Figure 8. Stable lights in southern hemisphere Africa, derived from 96 orbits of nighttime DMSP-OLS data.

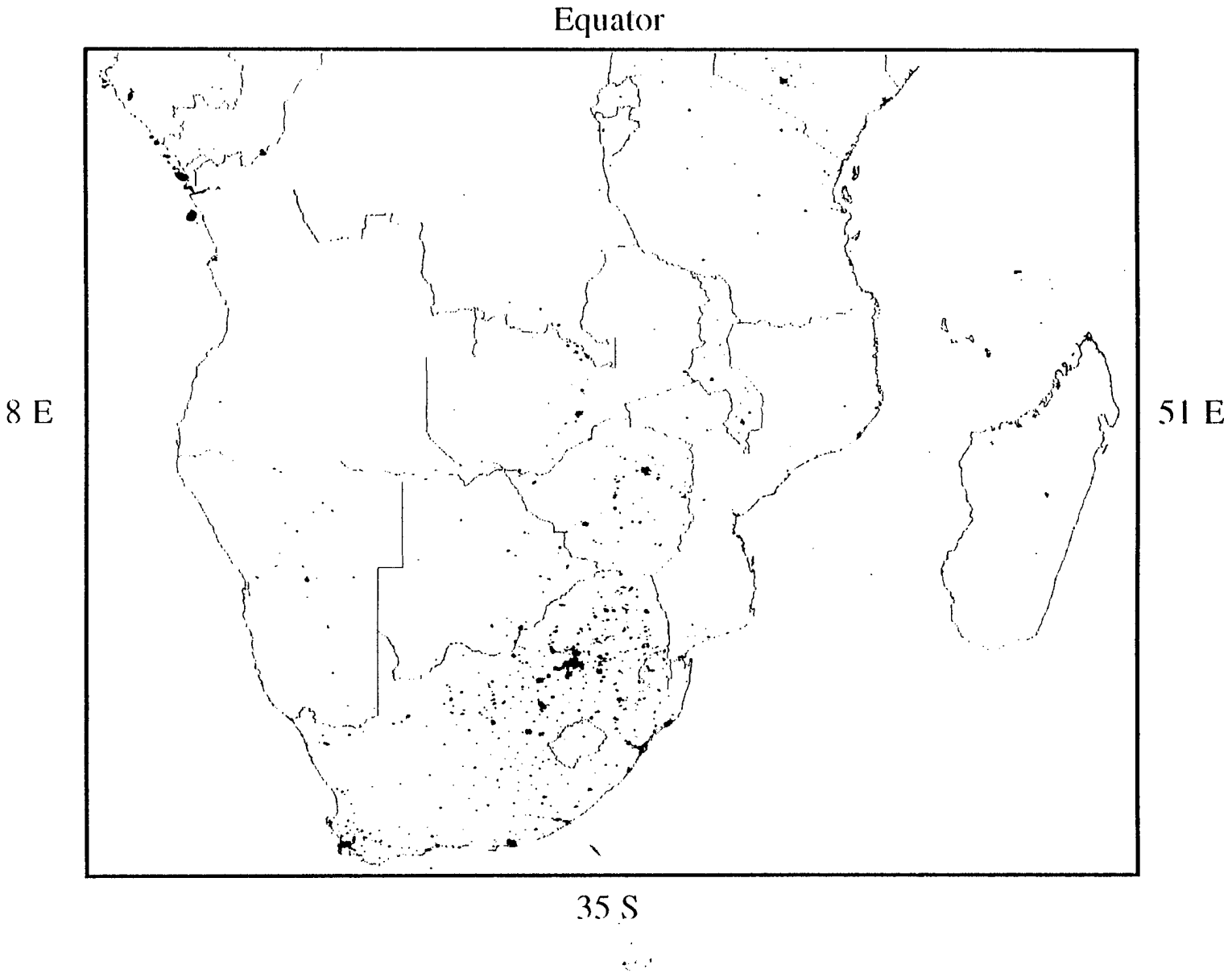

Figure 9. DMSP-OLS stable lights for an area surrounding Harare, Zimbabwe. Populated place lines from the Digital Chart of the World (DCW) are shown in white.

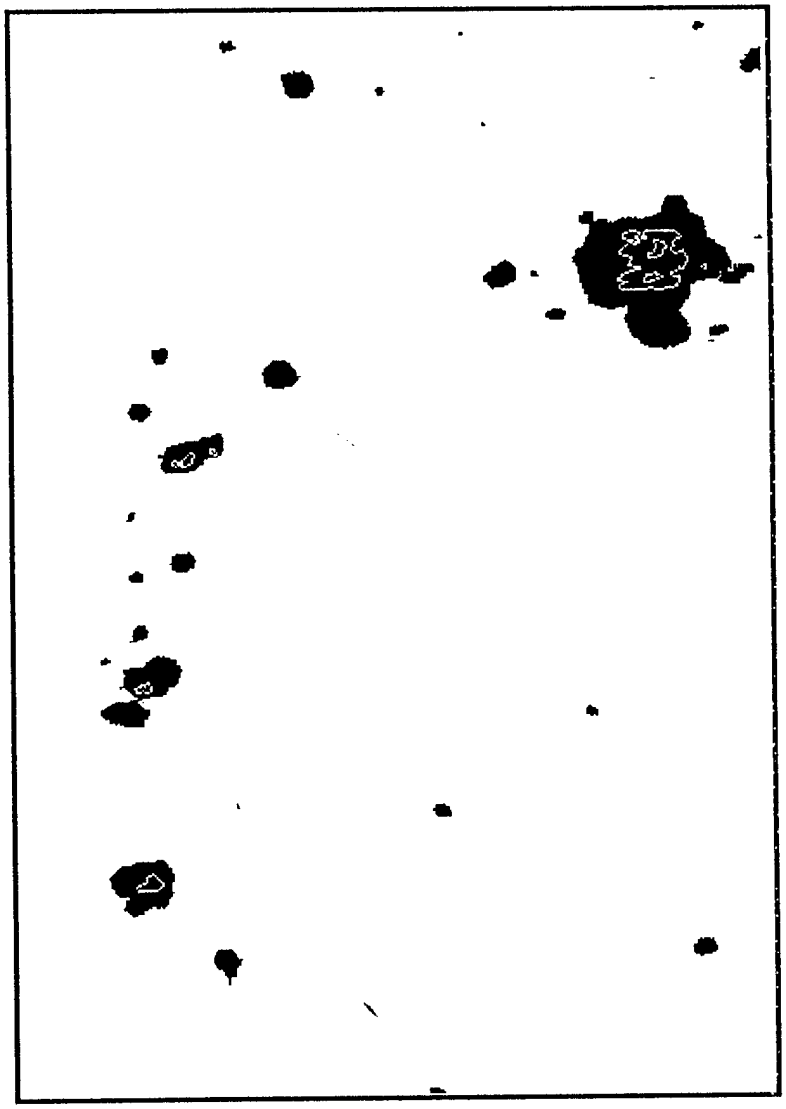

Figure 10. Nigthttime fires detected in southern hemisphere Africa on a single orbit acquired on September 18, 1992.

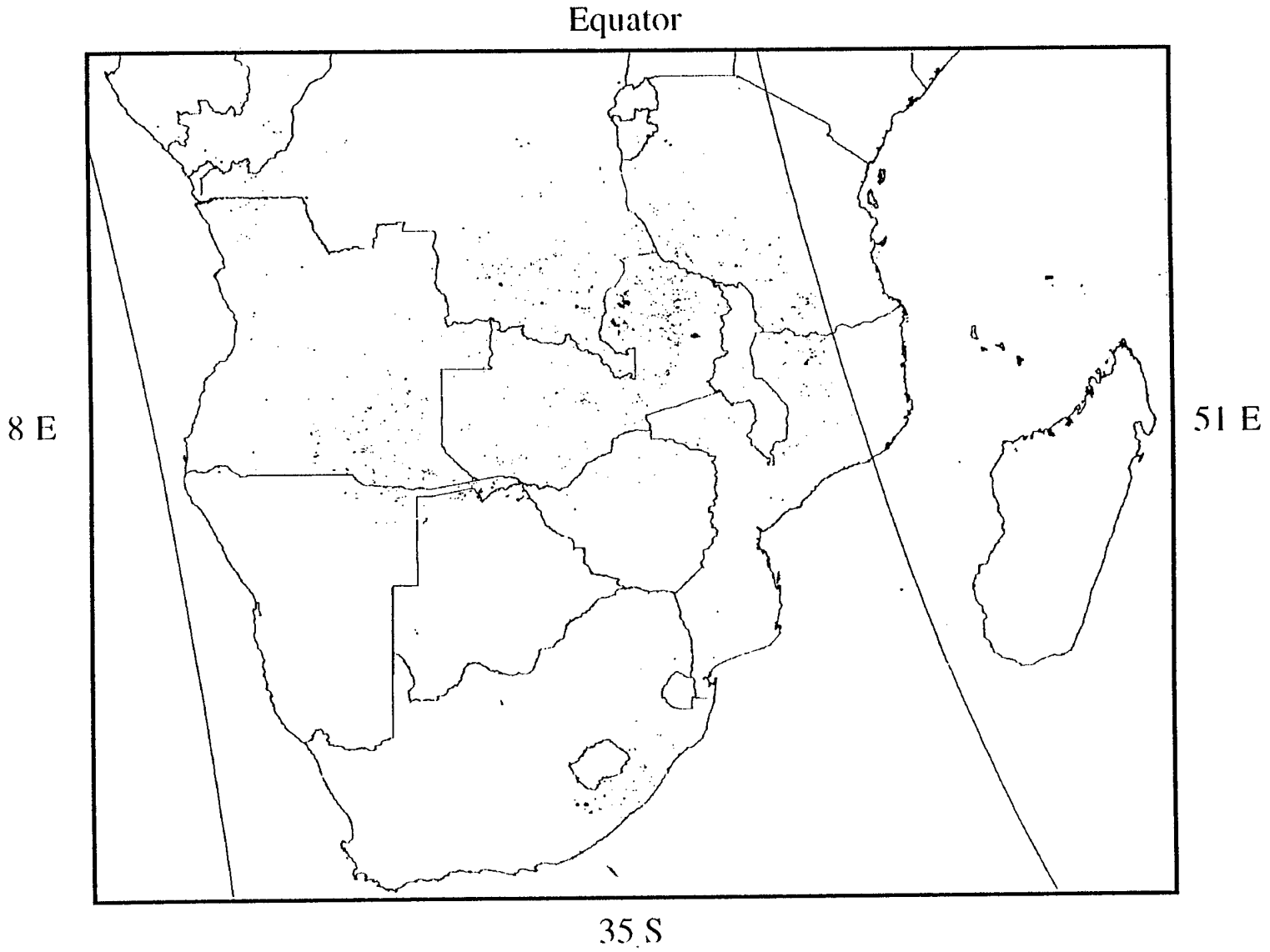

Figure 11. Nighttime fires detected in southern hemisphere Africa during six orbits acquired over three nights - September 18-20, 1992.

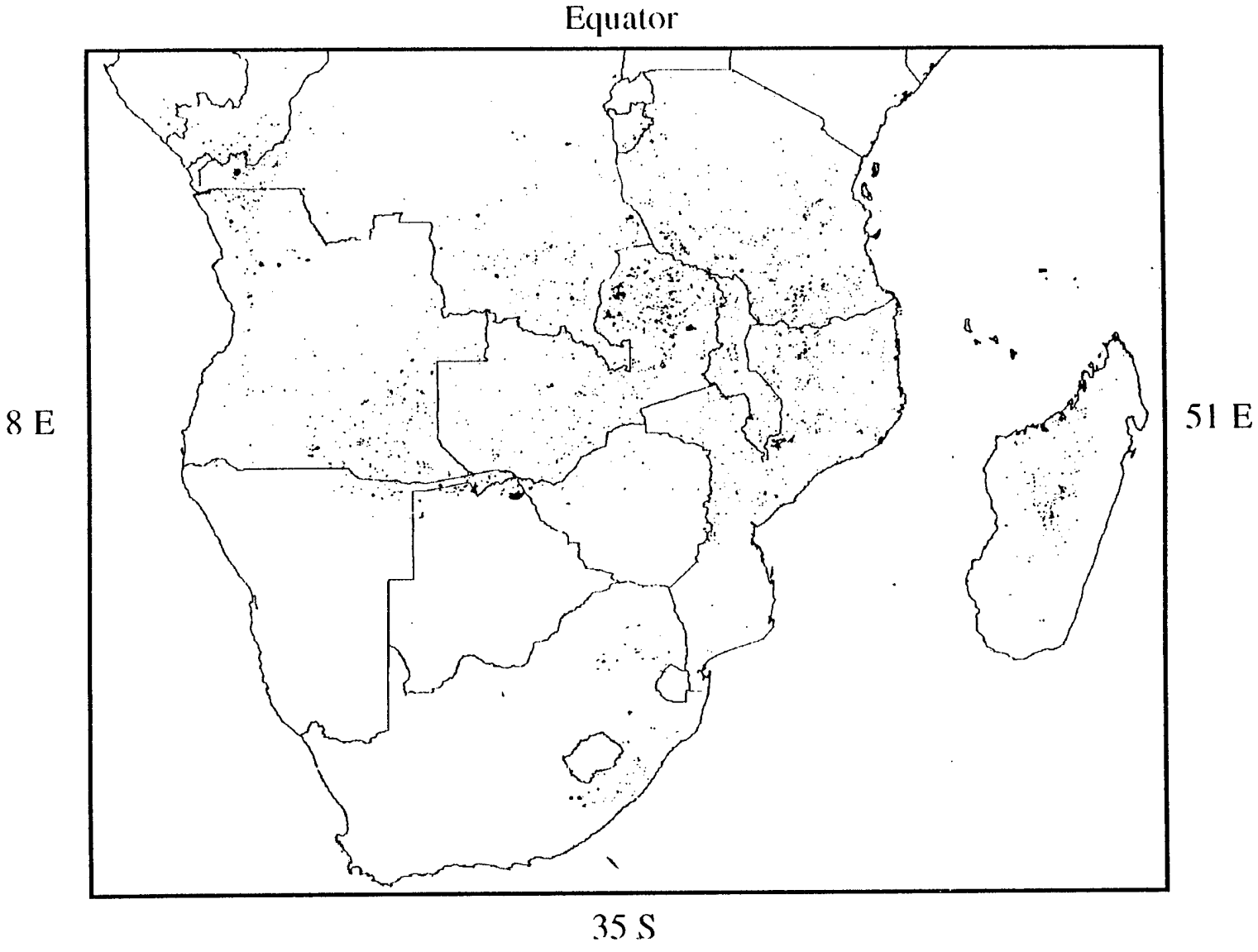

Figure 12. Smooth (2.7 km) versus fine (0.56 km) resolution DMSP-OLS data of fires in southern Sudan, December 7, 1994.

Smooth Data - 2.7 km Pixels

Fine Data - 0.56 km Pixels

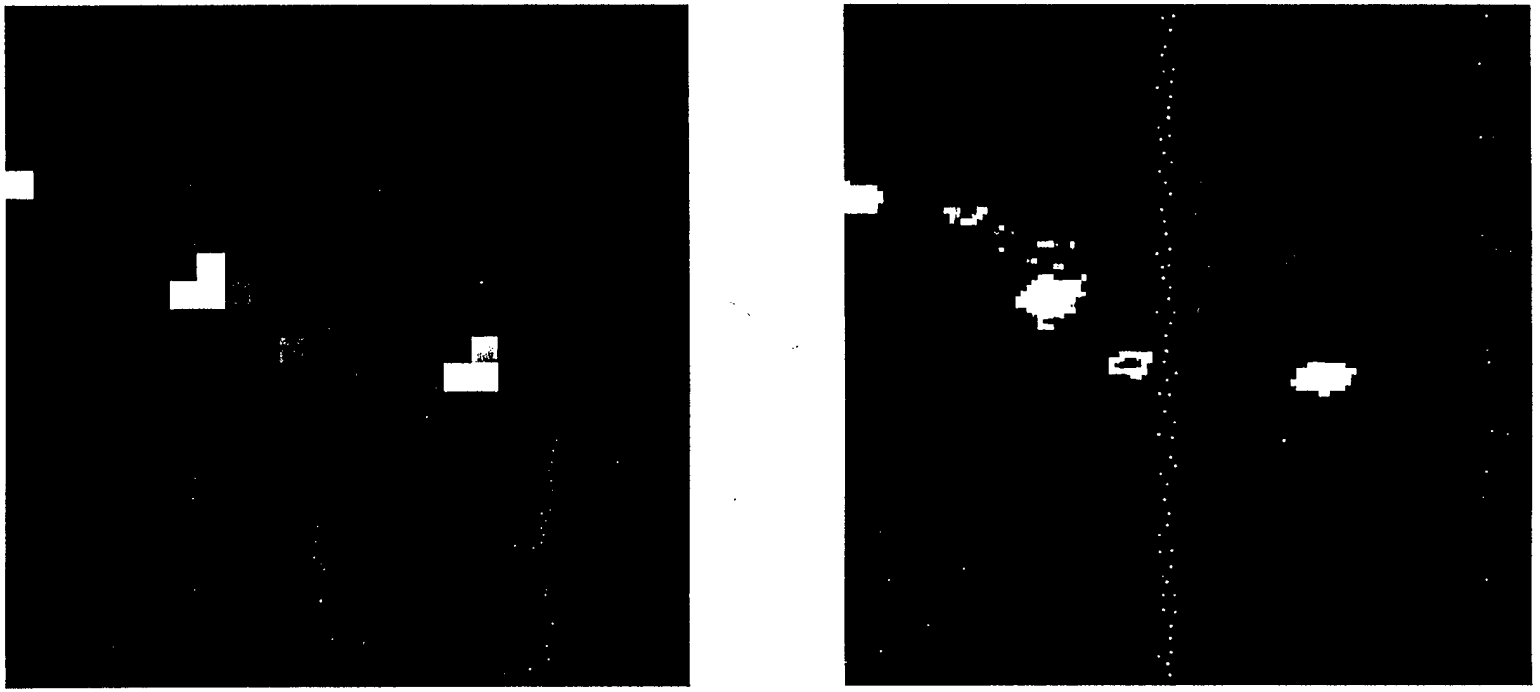

Figure 13. Carbon dioxide emissions from biomass burning in southern hemisphere Africa based on DMSP-OLS fire observations from September 18, 19, 20, 1992.

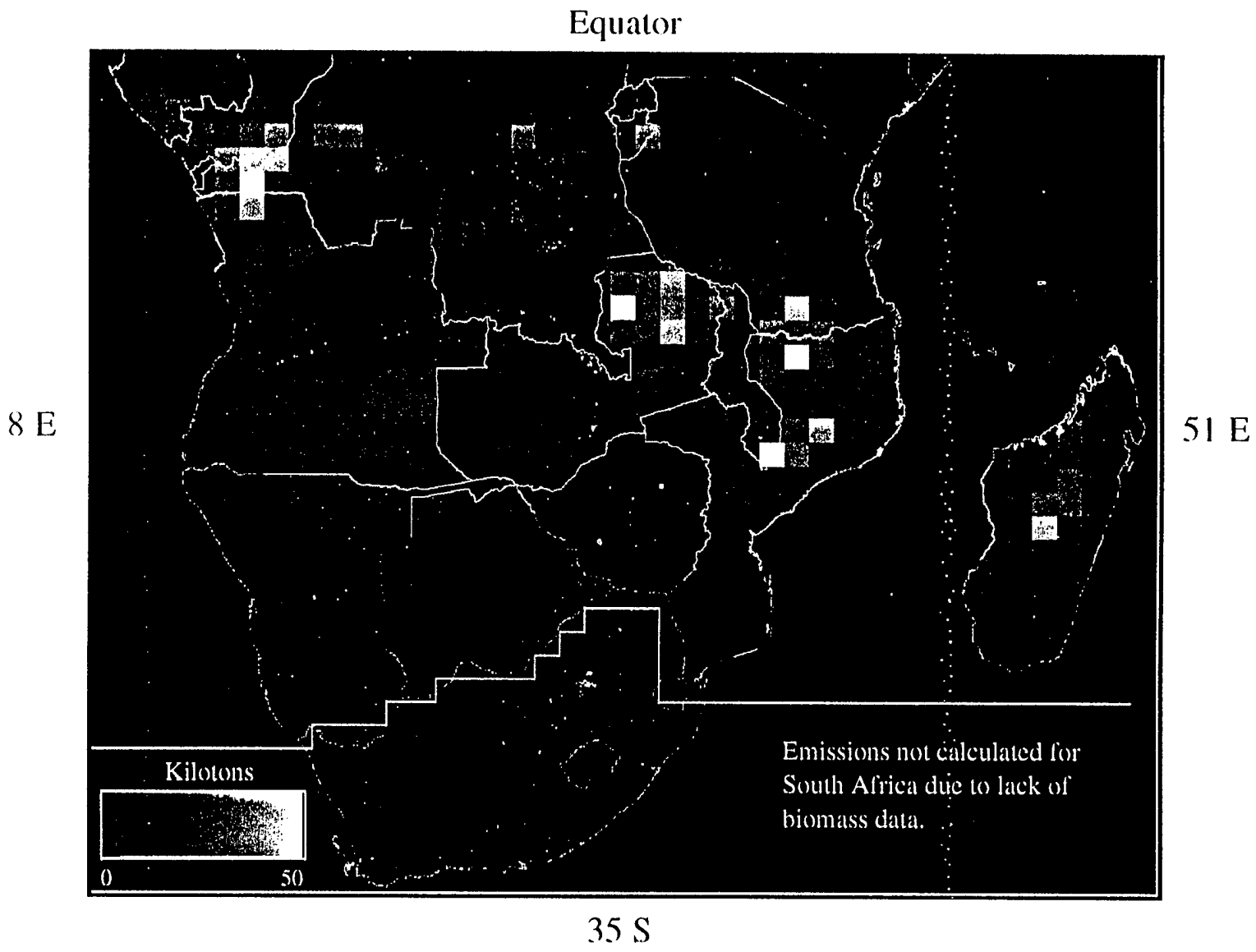

Figure 14. Effect of 1994 government "no-burn" edict in Madagascar on nighttime fires observed with DMSP-OLS data.